DOI: 10.1002/cphc.200900509

Hydrogen Radical Additions to Unsaturated Hydrocarbons and the Reverse β-Scission Reactions: Modeling of Activation Energies and Pre-Exponential Factors

Maarten K. Sabbe,[a] Marie-Françoise Reyniers,*[a] Michel Waroquier,[b] and Guy B. Marin[a]

The group additivity method for Arrhenius parameters is applied to hydrogen addition to alkenes and alkynes and the reverse β-scission reactions, an important family of reactions in thermal processes based on radical chemistry. A consistent set of group additive values for 33 groups is derived to calculate the activation energy and pre-exponential factor for a broad range of hydrogen addition reactions. The group additive values are determined from CBS-QB3 ab-initio-calculated rate coefficients. A mean factor of deviation of only two between CBS-QB3 and experimental rate coefficients for seven reactions in the range 300–1000 K is found. Tunneling coefficients for these reactions were found to be significant below 400 K and a correlation accounting for tunneling is presented. Application of the obtained group additive values to predict the kinetics for a set of 11 additions and β-scissions yields rate coefficients within a factor of 3.5 of the CBS-QB3 results except for two β-scissions with severe steric effects. The mean factor of deviation with respect to experimental rate coefficients of 2.0 shows that the group additive method with tunneling corrections can accurately predict the kinetics and is at least as accurate as the most commonly used density functional methods. The constructed group additive model can hence be applied to predict the kinetics of hydrogen radical additions for a broad range of unsaturated compounds.

1. Introduction

Addition of hydrogen radicals to alkenes and its reverse reaction, β-scission, are important elementary steps in radical processes such as polymerization, pyrolysis, steam cracking, partial oxidation, and combustion.[1] Therefore, the family hydrogen addition/β-scission reactions forms an indispensable part of any radical reaction network.

Reliable reactor optimization requires an accurate kinetic model based on elementary reactions. For radical chemistry, on which many of the world's largest scale chemical processes are based, the reactive nature of the radical intermediates results in huge reaction networks typically involving hundreds of species and thousands of elementary reactions.[2–4] Currently, most elementary reaction networks are automatically generated by using advanced algorithms for selection of the relevant reactions.[5–11] Sensitivity studies on these reaction networks point out that the main part of the uncertainty in product yields stems from inaccurate knowledge of kinetic data.[12,13] Therefore, accurate kinetic data are essential to obtain reliable process simulations. Moreover, if rate-based network-construction algorithms are applied,[14] accurate rate data are even more important, as inaccuracies can result in construction of an incomplete network that is not capable of grasping the underlying chemistry of the process.

A quantitative description of radical processes thus requires that rate parameters be known for all of the different reactions comprising the reaction network. However, it is very difficult to measure kinetic parameters for individual radical reactions experimentally, as these reactions are frequently coupled. Therefore, a variety of methods for predicting the rate of radical reactions has been developed. They range from correlating the activation energy to the reaction enthalpy, for example, Evans–Polanyi correlation and its variations,[15–17] to more sophisticated methods based on the structure of the transition state. Several of the latter methods are related to Benson group additivity.[18,19] Among these are: 1) the structural group contribution method of Willems and Froment,[20,21] in which correction terms on the Arrhenius parameters of a reference reaction account for structural differences between it and the considered reaction; 2) methods that calculate the thermochemistry of the transition state, such as that described by Sumathi et al.;[22–24] 3) the reaction class transition state theory developed by Truong et al.;[25,26] and 4) the group additive (GA) method for activation energies as described by Saeys et al.[27,28] Experimental determination of all kinetic and thermodynamic parameters required for these methods is not possible due to scarcity of experimental data. Moreover, experimental determination of rate constants often involves assuming a reaction scheme, which can induce a rather large scatter in the resulting reported kinetic data for a given reaction. Quantum chemical calculations can be applied to any reaction type, and extracting quan-

[a] Dr. M. K. Sabbe, Prof. Dr. M.-F. Reyniers, Prof. Dr. G. B. Marin
Laboratorium voor Chemische Technologie
Ghent University, Krijgslaan 281 S5, 9000 Gent (Belgium)
Fax: (+32) 9-264-5824
E-mail: mariefrancoise.reyniers@ugent.be

[b] Prof. Dr. M. Waroquier
Center for Molecular Modeling, Ghent University
Proeftuinstraat 86, B-9000 Gent (Belgium)

Supporting information for this article is available on the WWW under http://dx.doi.org/10.1002/cphc.200900509.

titative values of rate coefficients does not rely on assuming a reaction scheme. Therefore, the use of quantum chemistry to calculate rate coefficients for gas-phase radical reactions is particularly attractive, and the more recently developed parameterization schemes for addition of carbon-centered radicals and reverse β-scissions,[29] as well as for hydrogen abstraction,[22–26] are all based on first-principles calculations to determine the model parameters.

Although hydrogen addition is less commonly studied than hydrogen abstraction or non-hydrogen radical addition, rate coefficients for this family of reactions are included in many literature reviews on rate coefficients of radical reactions. In general, these reviews report not only experimental data but also predicted and extrapolated data. Hydrogen additions to hydrocarbons are included in, among others, the reviews of Baulch et al.[30,31] and Tsang,[32–35] which concentrate on combustion chemistry, and a review by Curran[36] that summarizes experimental work on the decomposition of C_1 to C_4 alkyl radicals through C–C and C–H β-scission reactions.

Hydrogen addition to ethene is widely studied both experimentally[37,38] and by ab initio methods. Ab initio studies at the early level of theory by Jursic[39] and Nguyen et al.[40] indicate troublesome determination of the transition state by DFT methods for this hydrogenation reaction and underprediction of the barrier to addition. Fischer and Radom also showed that DFT methods tend to underestimate the barriers for hydrogen additions.[41] In general, addition to the most substituted carbon atom is slower than addition to the less substituted atom,[41] based on enthalpic and entropic considerations, as well as on evaluation of the carbon atom with the highest spin density in the alkene triplet, which is the preferred site for radical attack.[42] Clarke et al.[43] studied the contribution of several properties to the barrier for hydrogen addition, revealing the dominant effect on the reactivity of the ionic state formed by transferring electron density from the alkene to the hydrogen atom. Using variational transition-state theory and master-equation analysis, Miller and Klippenstein[44,45] studied hydrogen addition to ethene, ethyne, and 1,3-butadiyne. They showed that for these reactions tunneling effects make a large contribution to the rate coefficient at lower temperatures that disappears above 1000 K, and that the largest difference between conventional and microcanonical variational transition-state theory is, even at 2500 K, limited to 19% for H + ethene, 28% for H + ethyne and 15% for H + 1,3-butadiyne. Both approaches yield results within 10% of each other at temperatures below 1000 K and the variational effect decreases with temperature. Based on a two-dimensional master equation analysis, Miller and Klippenstein[44] showed that, at 298 K, the reaction H + ethene already reaches the high-pressure limit at atmospheric pressure, while the rate coefficient of the highly pressure dependent addition to ethyne under these conditions is only about a factor of two below the high-pressure limit. The findings of Miller and Klippenstein[44,45] justify the approach used in this work, in which conventional transition-state theory is applied to determine the rates for a large set of reactions in the temperature range of 300–1300 K. Villa et al.[46–48] also showed the importance of including tunneling effects for hydrogen addition to ethene in describing the trends in kinetic isotope effects using variational transition-state theory. They reported that addition to the most deuterium substituted carbon atom is kinetically favored over the less substituted carbon atom.

In contrast to other reaction families, such as hydrogen abstraction, simple rate-prediction methods for hydrogen addition are scarce in the literature. The curve-crossing model of Clarke et al.[43] allows the barrier to be predicted but requires inclusion of ionic and covalent excited states and is, as such, less suited for implementation in automated network-generation software. Denisov[49–51] includes hydrogen addition reactions in a general prediction method for activation energies of radical addition based on the intersecting parabola model. The method includes addition to various substrates, including butadiene, styrene, triple bonds, C=O bonds, and acrylonitrile. However, due to its complexity this method is also less suited for implementation in automatic rate-prediction software. Moreover, both methods are limited to prediction of the activation energy and do not allow prediction of the pre-exponential factor. To the best of our knowledge, no structure–reactivity correlation covering a wide range of hydrogen additions to hydrocarbons is available in the literature.

Our aim was to determine a consistent set of group additive values (ΔGAV°) for prediction of activation energies and pre-exponential factors of hydrogen addition to a broad range of hydrocarbons and the reverse C–H β-scissions, in line with the recently reported group additive model for addition of carbon-centered radicals.[29] The computational approach involves conventional transition-state theory based on high-level CBS-QB3 ab initio calculations,[52] which has already shown its accuracy for similar radical reactions in previous work.[27–29,53] First, the computational method is validated for hydrogen additions by comparing the CBS-QB3 rate coefficients with computational and experimental data available in the literature. Next, rate coefficients are calculated for 34 reactions, from which 33 group additive values are derived, and a model to correct for tunneling effects is proposed for rate predictions at temperatures below 1000 K. Finally, the obtained group additive model is validated by comparing group-additive-predicted rate coefficients with ab-initio-calculated values and with experimental rate coefficients. The temperature range covered is 300–1300 K, which encompasses most chemical applications except combustion.

Computational Methods

Transition-State Geometry: Rate coefficients were calculated according to the methodology described by Saeys et al.,[54] based on the CBS-QB3 method of Montgomery et al.[52]. It is well known that DFT methods, and in particularly the B3LYP functional,[40,41] which is used for geometry optimization in the CBS-QB3 compound method, have difficulties in determining accurate transition-state geometries for hydrogen addition reactions. Therefore, the transition-state geometry was determined as described previously by Saeys et al.[54] First, the transition-state was optimized at the MPW1K/6-31G(d) level by using standard transition-state search algorithms provided by Gaussian 03.[55] From this geometry the C–

H_{MPW1K} bond length is extracted and is scaled by using the correlation proposed by Saeys et al.[54] to bring the MPW1K/6-31G(d) transition state geometries into accordance with IRCMax(CBS-QB3//B3LYP/6-311G(d,p)) geometries [Eq. (1)]:[56]

$$d(\mathrm{C{-}H_{IRCMax}}) = 0.4904\, d(\mathrm{C{-}H_{MPW1K}}) + 94.07\ \mathrm{pm} \quad (1)$$

Finally, the transition state is reoptimized while constraining the length of the forming C–H bond at the $C–H_{IRCMax}$ bond length determined by using Equation (1). Reoptimization is performed with the B3LYP/6-311G(d,p) method used for geometry optimization in the CBS-QB3 calculation. The obtained geometry is then used for calculation of the reaction barrier and the partition functions.

Rate Coefficients: Rate coefficients were calculated by using conventional transition-state theory (TST) in the high-pressure limit [Eq. (2)]:[57]

$$k_\infty(T) = \kappa(T)\frac{k_B T}{h}\frac{n_{\mathrm{opt},\ddagger} q_\ddagger^\ddagger}{n_{\mathrm{opt,A}} q_A n_{\mathrm{opt,B}} q_B} e^{-\frac{\Delta E(0\,K)}{RT}} \quad (2)$$

where q is the molecular partition function per unit volume, $\Delta E(0\ K)$ the electronic zero-point-corrected reaction barrier, and $\kappa(T)$ the transmission coefficient accounting for quantum mechanical effects. The term n_{opt} corrects for the number of optically active isomers, as the partition functions q pertain to a single enantiomer. The activation barrier at 0 K is determined with the CBS-QB3 complete-basis-set method of Montgomery et al.[52] All ab initio calculations were performed using the Gaussian 03 computational package.[55] Quantum tunneling coefficients $\kappa(T)$ were calculated by using the Eckart tunneling scheme,[58] as it has already proven its reliability for radical reactions.[59–61]

Partition functions q were calculated by using statistical thermodynamics based on the CBS-QB3 built-in B3LYP/6-311G(d,p) frequency calculation with a default scaling factor of 0.99. The partition functions were evaluated by using the rigid-rotor and harmonic oscillator (HO) approximation, assuming separability of translational, external rotational, rovibrational, and electronic contributions. Contributions of internal rotation to the rate coefficient are assumed to cancel out in the approximation that the internal rotations have similar contributions in reactant and transition state. This holds for hydrogen addition, since addition of a hydrogen atom does not introduce a new internal rotor in the transition state, no internal rotation occurs around the forming C–H bond, and, due to the early transition state for addition reactions, rotation around the breaking π bond is not yet possible. Only for β-scission might the HO approximation influence the rate coefficients, as rotation about the forming π bond is more hindered in the transition state than in the reactant radical. The deviation introduced by the harmonic-oscillator description of this rotation in the reactant radical is limited to, in the case of free rotation such as, for example, that of a methylene $–CH_2$ rotor, a factor of about two at 298 K and a factor of three at higher temperatures.

Arrhenius parameters were fitted to the ab-initio-calculated rate coefficient, that is, without inclusion of the tunneling coefficient κ, by using an Arrhenius fit with k sampled at intervals of 50 K between $T-100$ and $T+100$ K, where T is the temperature of interest. Calculation of the partition functions, the tunneling corrections, the rate coefficients and the Arrhenius parameters was fully automated.

Herein, the accuracy of the calculated rate coefficients is assessed by comparing the calculated and experimental rate coefficients. As a measure for the deviation the factor of deviation ρ, as applied in previous studies,[29,61,62] is defined by Equation (3):

$$\rho = \begin{cases} \frac{k_{calcd}}{k_{exptl}} & \text{for } k_{calcd} > k_{exptl} \\ \frac{k_{exptl}}{k_{calcd}} & \text{for } k_{exptl} > k_{calcd} \end{cases} \quad (3)$$

The factor ρ thus has a value greater than unity and gives a proper indication of the factor of difference between the two rate coefficients. It permits a mean factor of deviation $\langle\rho\rangle$ to be calculated by averaging over a set of reactions, which is not possible for the ratio of the rate coefficients.

Group Additivity Method: The group additivity model for prediction of activation energies and pre-exponential factors was described in detail previously.[27,29] Briefly, in the group additive model, the rate coefficient is expressed as Equation (4):

$$k = \kappa n_e k_{GA} = \kappa n_e \tilde{A} \exp(-\frac{E_a}{RT}) \quad (4)$$

where κ is the tunneling coefficient, n_e the number of single events, $\tilde{A}$ the single-event pre-exponential factor, and E_a the activation energy.

In the group additivity method, the transition state is written in terms of Benson groups (see Figure 1). In the Benson method, a group is defined as a polyvalent atom together with all of its ligands. Groups are denoted as $X\text{-}(A)_i(B)_j(C)_k(D)_l$, where X is the central atom surrounded by i A atoms, j B atoms, k C atoms, and l D atoms. To describe the reactions in this work, only hydrogen and carbon atoms are required, but different types of carbon atoms are distinguished: C_d and C_t for a doubly and triply bound carbon atoms, $C^\bullet$ for a carbon radical, and C_B for a carbon atom in a benzene ring. Although the adding hydrogen can, in principle, be regarded as a single-atom primary group it is not considered as a primary group in this work, as the adding radical is not varied within the family of reactions studied here.

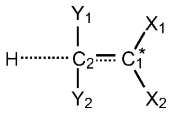

Figure 1. Transition state of a generic hydrogen addition depicting the numbering of the groups.

Extrapolating the common group additivity approximations[27,29] to hydrogen addition reactions, such as restriction to the primary groups, that is, the group centered on the C_1 and C_2 carbon atoms that are involved in bond formation and breaking, the activation energy E_a of a given reaction can then be written as Equation (5):

$$E_a(T) = E_{a,ref}(T) + \sum_{i=1}^{2} \Delta GAV^\circ_{E_a}(C_i) \quad (5)$$

where the activation energy is written as a sum of the reference activation energy $E_{a,ref}$ and group additive values ΔGAV°. In this notation, Δ denotes the difference between transition state and reactant, while "$^\circ$" indicates that the values are taken relative to the reference reaction. The reference reaction applied to this family of reactions is addition of a hydrogen radical to ethene (Figure 2).

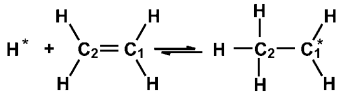

Figure 2. Reference reaction for group additive modeling of hydrogen additions.

Hence, the ΔGAV° in Equation (5) pertain to structural differences related to the attacked carbon atom, $\Delta GAV^{\circ}(C_2)$, and the formed radical, $\Delta GAV^{\circ}(C_1)$, of a given reaction and the reference reaction, as illustrated in Figure 1. The advantage of introducing a reference reaction is that most of the temperature dependence of the Arrhenius parameters can be accounted for by the reference reaction, while the ΔGAV° are largely temperature independent.

The practical implementation of the calculation of pre-exponential factors involves the single-event pre-exponential factor of the reference reaction $\tilde{A}_{ref}$, the primary group additive values ΔGAV°,and the number of single events n_e [Eq. (6)]:

$$\lg A(T) = \lg \tilde{A}_{ref}(T) + \sum_{i=1}^{2} \Delta GAV_A^{\circ}(C_i) + \lg n_e \qquad (6)$$

The number of single events n_e in Equation (6) is given by Equation (7):[63–65]

$$n_e = \frac{n_{opt,\ddagger}}{n_{opt,A} n_{opt,B}} \frac{\sigma_A \sigma_B}{\sigma_{\ddagger}} \qquad (7)$$

where n_{opt} is the number of optical isomers, and σ the total symmetry number of the molecule, that is, the product of the external and the internal symmetry numbers $\sigma_{int,i}$, the symmetry numbers of the internal rotations.

Since only the groups centered on C_1 and C_2, that is, primary groups, are considered, it is advisable to calculate the reverse rate coefficient from the ratio of the forward rate coefficient and the equilibrium coefficient, whereby the latter is predicted by thermochemical group additivity for reactants and products, in order to assure thermodynamic consistency during practical application of the group additive method.

Most group additive values presented in this work are determined from a single reaction for which only one ΔGAV° applies. For example, the ΔGAV° for the C_1-(C)-(H) group is determined from hydrogen addition to the unsubstituted carbon atom of propene and the reverse β-scission. The ΔGAV° for the activation energy is determined as the difference between the activation energy for the reaction with propene and the reference reaction, that is, the reaction with ethene. The ΔGAV° for the pre-exponential factor is determined as the difference of the single-event pre-exponential factor and the single-event pre-exponential factor of the reference reaction. Some ΔGAV° are determined from reactions for which multiple groups apply, in particular for additions to triple and allenic bonds. These reactions involve the C_{1t}-(C), C_{1t}-(C_d), and C_{1t}-(C_t) groups, which always occur in combination with a C_{2t}-(X) group (X = H, C, C_d, or C_t), and the $C_{1,allene||}$-(C)-(H) and $C_{1,allene||}$-($C)_2$ groups, which always occur together with the $C_{2,allene}$ group. For example, the group $C_{1,allene||}$-($C)_2$ is determined from the reaction with 3-methylbuta-1,2-diene:

for which the group $C_{2,allene}$ describes addition to an allenic carbon atom, and the group $C_{1,allene||}$-($C)_2$ substitution at the formed radical.

Tunneling Correction: The aim of the group additivity method is on-the-fly calculation of the rate coefficients of all reactions in a large radical network, based on a set of available ΔGAV° for activation energies and pre-exponential factors. As such, its main purpose is to avoid the need for costly quantum chemical calculations, in particular for the larger reactions in the network. However, the ΔGAV° as such do not include quantum mechanical tunneling effects, which can be important, in particular at lower temperatures. In general, knowledge of the tunneling contribution for a particular reaction in the reaction network requires knowledge of the energy along the reaction path, and for more accurate treatments even the Hessian, which can be computationally very costly to obtain. Therefore, a method to correct the group additively calculated rate coefficients for quantum mechanical tunneling effects that avoids explicit calculation of the tunneling coefficients for all the reactions present in the reaction network was developed.

As pointed out by Truong et al.,[59] reactions belonging to the same family have the same reactive moiety and are expected to have similarities in their potential-energy surface along the reaction path. Therefore, information on the potential-energy surface along the reaction path for the reference reaction, which is usually the "smallest" reaction in the family, can be transferred to the calculation of tunneling contributions to the rate of larger reactions without having to evaluate their tunneling coefficients explicitly. In the frame of reaction-class transition-state theory as developed by Truong,[59] the tunneling contribution to the rate coefficient of a given reaction in the family is determined by multiplying the temperature-dependent tunneling coefficient of the reference reaction by a temperature-dependent function [Eq. (8)]:

$$\kappa = \kappa_{ref}(T) f(T) \qquad (8)$$

Truong et al. successfully applied this approach to calculate rates of hydrogen abstraction from a limited set of alkanes and alkenes by hydrogen and methyl radicals, by using separate expressions for $f(T)$ for different abstraction sites.[26,60,66,67]

To apply Equation (8) in the framework of group additivity, a correlation $f(T)$ should be determined for every group or combination of groups. The advantage of the approach of Equation (8) is that the tunneling coefficient for the reference reaction can be determined at a higher level and transferred to the other reactions by using the correlation for κ/κ_{ref}. The drawback is that two correlations must be evaluated, one expressing the temperature dependence of the tunneling coefficient of the reference reaction, and the other the ratio κ/κ_{ref}, depending on the groups present in the transition state.

Although a similar procedure can be implemented within the framework of the group additivity method, in this work a more pragmatic approach was investigated to obtain tunneling corrections for reactions belonging to the same family, based on properties that are easily accessible during practical application of the group additive method. The main factors controlling tunneling in the zero-curvature approximation, that is, the net electronic tunneling barrier and the imaginary frequency in the transition state, are not accessible during practical application of the group additive model for rate prediction. However, due to the exothermicity of the hydrogen addition reactions, the activation energy of addition provides a good approximation for the net electronic tunneling barrier. Within this approximation, the tunneling contribution

to the rate coefficient of a reaction in the family can be expressed as function of the temperature and the activation energy for the addition reaction, $\kappa(T,E_{a,add})$. The advantage of this approach is that tunneling corrections for all reactions for which ΔGAV° are available can be modeled very easily. Here an appropriate expression for $\kappa(T,E_{a,add})$ is derived. The results of this approach and that using Equation (8) are compared.

2. Results and Discussion

In this section, first the reliability of the computational method is illustrated by comparison with high-level quantum chemical data available in the literature and with experimental values. Next, the rate coefficients are presented and the activation energies and pre-exponential factors, which are derived from an Arrhenius fit to the ab-initio-calculated rate coefficients, that is, without tunneling contributions, are discussed. Then, the group additive values are presented and an expression to account for tunneling effects is derived. Finally, the use of the group additive model is illustrated and validated by comparing the predictions with ab-initio-calculated values and with experimental rate coefficients.

2.1. Validation of the Computational Method

Previous level-of-theory studies showed that the CBS-QB3 method yields accurate data for similar radical reactions. Here the reliability of the CBS-QB3 method for hydrogen addition reactions is illustrated. Table 1 compares the CBS-QB3 data with the QCISD(T) quantum chemical data, extrapolated to the infinite basis-set limit, as reported by Miller and Klippenstein,[44,45] for the activation energy barriers at 0 K, $\Delta E(0\,K)$, the reaction energies at 0 K, $\Delta_r E(0\,K)$, and high-pressure-limit rate coefficients of the reactions H + ethene, H + ethyne, and H + 1,3-butadiyne. The CBS-QB3 barriers are systematically lower than the QCISD(T)/∞ values by 1–3 kJ mol^{-1}, and the largest deviation of 2.8 kJ mol^{-1} is found for addition to 1,3-butadiyne, Klippenstein and Miller had to reduce the barrier by 2.1 kJ mol^{-1} to bring the rate coefficient into agreement with experimental measurements.[68] The reaction energies are also lower by 1–4 kJ mol^{-1}, except for addition to ethene. Due to the lower CBS-QB3 barriers, the CBS-QB3 rate coefficients are slightly larger than the QCISD(T)/∞ values, by 10–70% for addition to ethene and ethyne, and by up to a factor of three at 300 K for addition to 1,3-butadiyne. All differences between the rate coefficients can be attributed to differences in the reaction barrier. Miller and Klippenstein already showed variational effects to be small for these reactions (max. 15% at 2500 K). Summarizing, the CBS-QB3 results of this work agree well with those of other high-level calculations in the literature.

Table 2 compares rate coefficients obtained using CBS-QB3 with experimental rate coefficients taken from the NIST Chemical Kinetics Database,[69] where available. The set of experimental reference data includes only data indicated by NIST as "absolute rate value measured directly", "experimental value and limited review", "derived from detailed balance/reverse rate", and "extensive literature review". For the last-named category values indicated to be estimations were excluded. This yielded seven reactions for which the calculations could be compared to experimental reference data at 300, 600, and 1000 K (see Table 2). The experimental references and respective rate coefficients for these seven reactions are given in Table S1 of the Supporting Information. The deviation ratios k_{calcd}/k_{exptl} and the factor of deviation ρ for each experimental reference can be

Table 1. Comparison of the reaction barrier at 0 K $\Delta E(0\,K)$, the reaction energy at 0 K $\Delta_r E(0\,K)$, and the high-pressure rate coefficient with the respective QCISD(T)/∞ values obtained by Miller and Klippenstein.[42,43]

Reaction	$\Delta E(0\,K)$ [kJ mol^{-1}]		$\Delta_r E(0\,K)$ [kJ mol^{-1}]		$k_{\infty,\infty}$ [m^3 mol^{-1} s^{-1}]		
	CBS-QB3	QCISD(T)	CBS-QB3	QCISD(T)	T [K]	CBS-QB3	QCISD(T)
H + 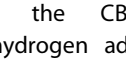	10.2	11.8[a]	−144.7	−146.4	300	1.0×10^6	5.9×10^5
					600	7.4×10^6	5.1×10^6
					1000	2.4×10^7	1.7×10^7
H + 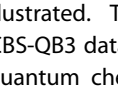	16.6	17.9[a]	−146.3	−145.1	300	3.3×10^5	2.5×10^5
					600	6.8×10^6	5.8×10^6
					1000	3.1×10^7	2.7×10^7
H + 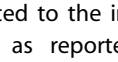	9.3	12.1[b]	−182.8	−178.7	300	5.6×10^6	1.5×10^6
		(10.0)[c]			600	2.7×10^7	1.4×10^7
					1000	6.9×10^7	4.2×10^7

[a] Ref. [42]. [b] Ref. [43]. Value obtained from the QCISD(T)/∞ calculation. [c] Value obtained after reducing the barrier height by 2.1 kJ mol^{-1} to bring the rate coefficients into agreement with the experimental measurement of Nava et al.[67]

Table 2. Experimental validation: comparison of ab-initio-calculated rate coefficients (including tunneling) with experimental values based on ρ factors as defined in Equation (3), averaged out per reaction.

No.	Reaction	$\langle\rho\rangle$ for addition			$\langle\rho\rangle$ for β-scission		
		300 K	600 K	1000 K	300 K	600 K	1000 K
1	H + 	1.4	1.5	1.6	1.4	1.5	1.8
2	H + 	2.7				2.9	1.9
3	H + 	1.4	1.3	1.9	3.1	4.9	2.0
4	H + 	1.5	1.6	2.4	2.2	1.2	1.2
5	H + 	1.1	1.9	2.9	1.2	1.4	2.3
6	H + 	2.4					
7	H +	1.4	1.1	1.3	3.7	1.3	1.4
	$\langle\rho\rangle$	1.7	1.5	2.0	2.3	2.2	1.8
	$\langle\rho\rangle_{mean}$	1.9					

retrieved from Tables S2 and S3 of the Supporting Information, while the mean factors of deviation $\langle\rho\rangle$ averaged per reaction are listed in Table 2.

From Table 2 it is clear that, also for hydrogen addition and β-scission, the CBS-QB3 method performs very well. For additions, the reaction-averaged factors of deviation $\langle\rho\rangle$ are smaller than three for all reactions. For β-scissions, a deviation larger than three is only observed for the β-scission of a primary propyl radical to give propene (Table 2, entry 3), mainly due to deviation from the 600 K experimental reference of Mintz and Leroy,[70] and for β-scission of a *tert*-butyl radical yielding isobutene (Table 2, entry 7).

The mean factor of deviation averaged over the different temperatures and reactions is 1.7 for the additions and 2.1 for the β-scissions, yielding a value of 1.9 on average for this family of reactions. Hence, for hydrogen additions, the CBS-QB3 approach yields even better results than for other families of reactions. For addition of carbon-centered radicals[62] a mean factor of deviation of 3 was found, while for hydrogen abstractions[61] a mean factor of difference of 5.8 was found, which, however, was mainly determined by large deviations at 300 K.

2.2. Rate Coefficients

The rate coefficients including tunneling contributions at 300 K for hydrogen additions and β-scissions evaluating the influence of substituents at C_1 can be found in Table 3, and for the reactions evaluating the influence of substituents at C_2 in Table 4. Kinetic parameters at 600 and 1000 K, as well as the parameters characterizing the transition state, applied symmetry numbers, number of optical isomers and number of single events can be found in Tables S4–S6 of the Supporting Information. The transition-state geometries are also reported in the Supporting Information.

The resulting rate coefficients for addition range from 10^2 to 10^7 $m^3 mol^{-1} s^{-1}$ at 300 K. The reactions evaluating the influence at C_1 are much faster than the second set in which the substituents on the C_2 carbon atom are varied, in agreement with the findings that the unsubstituted carbon atom is the kinetically most favorable site for radical attack.[41] The fastest reactions are the additions to the terminal carbon atom of 1,3-butadiene compounds (Table 3, reactions 4–6); the slowest reaction is addition to the phenyl substituted carbon atom of styrene yielding the 2-phenyleth-1-yl radical (Table 4, reaction 28).

For β-scissions, whose rate coefficients range from 10^{-32} to 10^{-9} s^{-1} at 300 K, the kinetics are dominated by the strong en-

Table 3. Tunneling coefficients, pre-exponential factors, activation energies, rate coefficients (including tunneling contributions), and reaction enthalpies for hydrogen additions and β-scissions, evaluating the influence of substituents at the C_1 carbon atom. The Arrhenius parameters were determined as described in the Computational Methods section (E_a and $\Delta_r H^\circ$ in kJ mol^{-1}, 300 K).

No.			$H^\cdot + H_2C{=}C(R_1)R_2$			κ	Addition			β-scission			$\Delta_r H^\circ$
							lg A	E_a	k_κ [$m^3 mol^{-1} s^{-1}$]	lg A	E_a	k_κ [s^{-1}]	
1	H	+		⇄		1.63	7.612	10.4	1.0×10^{6}	12.790	156.3	6.1×10^{-15}	−145.9
2	H	+		⇄		1.48	7.328	8.0	1.3×10^{6}	13.245	154.2	3.7×10^{-14}	−146.2
3	H	+		⇄		1.32	7.379	5.5	3.5×10^{6}	13.234	151.4	9.8×10^{-14}	−145.9
4	H	+		⇄		1.22	7.577	3.3	1.2×10^{7}	13.507	197.2	1.8×10^{-21}	−193.9
5	H	+		⇄		0.83	7.313	1.3	1.0×10^{7}	12.942	195.1	7.8×10^{-22}	−193.8
6	H	+		⇄		–	6.967	0	9.3×10^{6}	12.852	231.2	3.9×10^{-28}	−232.4
7	H	+		⇄		1.40	7.275	4.9	3.7×10^{6}	13.101	192.3	5.8×10^{-21}	−187.4
8	H	+		⇄		1.22	7.324	3.4	6.6×10^{6}	13.187	191.8	7.5×10^{-21}	−188.4
9	H	+		⇄		0.49	7.278	0.7	7.0×10^{6}	13.263	218.4	8.4×10^{-26}	−217.7
10	H	+		⇄		1.04	7.261	2.1	8.1×10^{6}	12.283	218.8	1.6×10^{-26}	−216.7
11	H	+		⇄		1.54	6.718	12.5	5.4×10^{4}	13.282	195.3	2.9×10^{-21}	−182.8
12	H	+		⇄		1.42	7.169	10.1	3.7×10^{5}	12.735	190.4	5.4×10^{-21}	−180.3
13	H	+		⇄		1.70	7.600	11.4	7.0×10^{5}	13.200	164.3	6.7×10^{-16}	−152.9
14	H	+		⇄		1.60	7.415	14.4	1.3×10^{5}	14.043	257.9	2.2×10^{-31}	−243.5
15	H	+		⇄		1.96	7.224	10.9	4.2×10^{5}	13.109	255.8	7.3×10^{-32}	−244.9
16	H	+		⇄		1.88	7.802	15.1	2.8×10^{5}	13.638	164.9	1.6×10^{-15}	−149.8
17	H	+		⇄		1.74	7.368	8.6	1.3×10^{6}	13.789	201.2	9.9×10^{-22}	−192.6
18	H	+		⇄		2.04	8.144	9.8	5.6×10^{6}	13.091	193.5	5.1×10^{-21}	−183.7

Table 4. Tunneling coefficients, pre-exponential factors, activation energies, rate coefficients (including tunneling contributions), and reaction enthalpies for hydrogen additions and β-scissions, evaluating the influence of substituents at the C_2 carbon atom. The Arrhenius parameters were determined as described in the Computational Methods section (E_a and $\Delta_r H^\circ$ in kJ mol^{-1}, 300 K).

No.	H• + 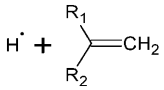			κ	Addition			β-scission			$\Delta_r H^\circ$
					lg A	E_a	k [m^3 mol^{-1} s^{-1}]	lg A	E_a	k [s^{-1}]	
19	H + 	⇄		1.97	7.123	14.7	7.2×10^{4}	13.095	148.1	4.0×10^{-13}	−133.4
20	H + 	⇄		2.10	6.885	18.4	1.0×10^{4}	12.725	142.8	1.5×10^{-12}	−124.4
21	H + 	⇄		2.03	7.479	16.8	7.3×10^{4}	12.916	135.0	5.2×10^{-11}	−118.2
22	H + 	⇄		2.15	7.005	20.2	6.6×10^{3}	12.513	131.2	1.0×10^{-10}	−111.0
23	H + 	⇄		2.34	6.814	23.0	1.5×10^{3}	12.345	130.9	8.4×10^{-11}	−107.9
24	H + 	⇄		2.20	7.153	17.9	2.4×10^{4}	12.684	140.7	3.4×10^{-12}	−122.8
25	H + 	⇄		2.38	6.970	22.9	2.3×10^{3}	12.575	138.8	6.1×10^{-12}	−115.9
26	H + 	⇄		2.50	7.105	25.2	1.3×10^{3}	12.601	126.6	9.0×10^{-10}	−101.4
27	H + 	⇄		2.68	7.086	27.9	4.5×10^{2}	12.504	133.0	5.9×10^{-11}	−105.1
28	H + 	⇄		2.19	6.658	26.0	3.0×10^{2}	12.609	151.6	3.6×10^{-14}	−125.6
29	H + 	⇄		2.07	6.827	25.7	4.7×10^{2}	12.578	147.0	2.0×10^{-13}	−121.3
30	H +	⇄		2.42	7.666	19.3	4.9×10^{4}	14.008	257.2	4.1×10^{-31}	−237.9
31	H + 	⇄		2.09	8.179	17.1	3.3×10^{5}	13.556	166.0	9.4×10^{-16}	−148.9
32	H + 	⇄		2.10	7.545	21.3	1.4×10^{4}	13.496	155.3	6.0×10^{-14}	−134.0
33	H + 	⇄		2.15	7.412	21.8	8.9×10^{3}	14.035	167.7	1.5×10^{-15}	−145.9
34	H +	⇄		2.37	8.094	25.8	9.5×10^{3}	13.382	158.7	1.3×10^{-14}	−132.9

dothermicity of the reactions. The slowest reaction is β-scission of the 3-methylbut-1-en-3-yl radical into 3-methylbuta-1,2-diene (Table 3, reaction 15), as formation of allenic moieties from allylic radicals are the most endothermic reactions of the whole set. The fastest reaction is formation of resonance-stabilized 2-ethynylbuta-1,3-diene (Table 4, reaction 26), which is the least endothermic reaction. Clearly, the rates of the strongly endothermic β-scissions are determined primarily by the reaction enthalpy.

Despite the very light hydrogen atom, the influence of tunneling on the rate coefficients is rather small due to the very low tunneling barriers. The tunneling coefficients for the reactions of Tables 3 and 4 range between 0.49 and 2.7 at 300 K. For two reactions reflection occurs: hydrogen addition to 2-methylbuta-1,3-diene (Table 3, reaction 5) and to 2-ethynylbuta-1,3-diene (Table 3, reaction 9) are almost barrierless with extremely low electronic barriers of 0.6 and 0.1 kJ mol^{-1}. For the barrierless addition to 2-ethenylbuta-1,3-diene (Table 3, reaction 6) no transmission coefficient was taken into account due to convergence problems, though reflection can be expected.[71] Despite the small corrections, tunneling coefficients should definitely be taken into account below 500 K, since the effects are greater than 50%. For temperatures of 500 K and higher, the contribution of tunneling is limited to 50% and at 1000 K the largest tunneling coefficient reduces to a negligible 1.08.

2.3. Arrhenius Parameters

The Arrhenius parameters at 300 K are given in Table 3 for reactions evaluating the influence of substituents at C_1, and in Table 4 for the reactions evaluating the influence of substituents at C_2. The reported Arrhenius parameters were fitted to the ab-initio-calculated rate coefficients without tunneling contributions.

For additions to terminal carbon atom C_2 in which the substituents at C_1 are varied (Table 3), the pre-exponential factors lg(A/m^3 mol^{-1} s^{-1}) range between 6.7 and 8.1, with the lowest value for addition to styrene (Table 3, reaction 11) and the highest to the addition to linear 1,3-butadiyne (Table 3, reaction 18). The substituents at C_1 have little effect on the pre-exponential factor for addition, except for additions to triple bonds, for which an increased pre-exponential factor is observed. The activation energies for the additions of Table 3 range between 0 and 15 kJ mol^{-1}. Many of the reactions have very low activation energies, as stabilization of the formed radical by the C_1 substituents through resonance and/or hyperconjugation lowers the activation energy. Addition to 2-ethenylbuta-1,3-diene (Table 3, reaction 6) forming a strongly resonance-stabilized radical is found to be barrierless.

For additions in which the substituents on the attacked carbon atom C_2 are varied (Table 4) the rate-decreasing effect of the substituents is reflected in a decrease in the pre-expo-

nential factor and an increase in the activation energy compared to addition to the unsubstituted end in Table 3. The only exceptions are additions to triple bonds, in particular hydrogen addition to ethyne and 1,3-butadiyne, for which pre-exponential factors are about an order of magnitude larger than the other values. For these reactions, loss of the molecular linearity on transition-state formation results in a higher activation entropy. The activation energies range between 15 and 28 kJ mol^{-1}, which is about 15 kJ mol^{-1} higher than for additions to the unsubstituted carbon atom, mainly due to reduced stabilization of the forming radical and increased steric hindrance in the transition state.

An Evans–Polanyi model for these activation energies, corrected for the electrophilic effects in the transition state by using the polar factors introduced by Fischer and Radom,[41] is presented in the Supporting Information. The results are in accordance with charge transfer to the hydrogen radical in the transition state, as identified by Clarke et al.[43] In general, the electrophilic influence is much smaller for hydrogen addition to the substituted C_2 atom (Table 4) than for the addition to the unsubstituted C_2 atom, but a quantitative correlation of this effect that is valid for all of the reactions in Tables 3 and 4 is not straightforward. Similar observations concerning the use of a combination of an Evans–Polanyi relation and polar factors describing the reactivity trends have been made previously for additions of carbon-centered radicals.[29]

For the β-scissions in which the substituents at the forming radical center are varied (see Table 3), the values of lg(A/s^{-1}) vary between 12.2 and 14.1 for the β-scission yielding 2-ethynylbut-1-en-3-yne (reaction 10 in Table 3) and the β-scission forming 1,2-butadiene (reaction 14 in Table 3), respectively. The presence of substituents at the forming radical center increases the pre-exponential factor for β-scission; all but two reactions in Table 3 have a larger pre-exponential factor than that of the β-scission of the unsubstituted ethyl radical. The activation energies are very large for this family of reactions, up to 258 kJ mol^{-1} for β-scission of a secondary allylic radical forming 1,2-butadiene (reaction 14 in Table 3). For these reactions, the activation energies are clearly dominated by the strong endothermicity. The only exceptions are the activation energies for the β-scission reactions yielding propene (reaction 2 in Table 3) and isobutene (reaction 3 in Table 3), which are lower than the activation energy of the β-scission forming ethene (reaction 1 in Table 3), while the reaction enthalpy remains about the same. The same holds for the addition reactions, for which the activation energies are lower than for addition to ethene. Apparently, the methyl substituents stabilize the transition state more than the radical in these reactions.

Finally, the effect on the β-scission kinetics of substituents on the C_2 carbon atom (see Table 4) is discussed. These substituents have only a small effect on the pre-exponential factor, and most lg$A$ values are similar to that for β-scission of the ethyl radical (lg(A/s^{-1}) = 12.3–13.1), except for β-scissions yielding allenic and triple bonds (reactions 30–34 in Table 4), for which lg(A/s^{-1}) ranges from 13.3 to 14. With the exception of the β-scissions yielding allene and triple bonds, the activation energies range between 126 and 152 kJ mol^{-1}. In general, substituents at the C_2 atom result in an increase of the activation energy, as opposed to their effect on the addition path, where they decrease the rates. The C_2 substituents stabilize the formed alkene more than the radical, and this decreases the β-scission activation energy with respect to β-scission yielding ethene. For the β-scissions yielding allene and triple bonds, higher activation energies occur, up to 257 kJ mol^{-1} for decomposition of an allylic radical to allene (reaction 30 in Table 4).

The difference in behavior between β-scissions yielding triple bonds and β-scissions yielding alkenes can be understood as follows. For the β-scissions forming alkenes π-bond formation involves a transition from a single to a double bond, and double-bond formation strongly reduces the internal mobility in the transition state relative to the product radical. The transition state is late from the viewpoint of β-scission, which means that rotation about the forming π bond is already severely inhibited. For formation of triple bonds through β-scission of a vinylic radical that already contains a double bond, there is no loss in mobility due to increased hindrance of rotation around the forming bond. Also, the presence of several low-frequency modes indicates an increase in mobility on proceeding from the vinylic radical to the transition state. The increase in mobility on transition-state formation results in a higher pre-exponential factor than for the β-scission reactions yielding alkenes. Albeit to a lesser extent, this is also the case for the β-scission of resonance-stabilized radicals, due to the additional constraints on the internal mobility of the radical imposed by the resonance. A very pronounced case is the β-scission of an allyl radical with the formation of allene (reaction 30 in Table 4), for which the pre-exponential factor for β-scission is two orders of magnitude larger than for β-scission of the ethyl radical yielding ethene. In this reaction, not only does the allyl radical have low entropy due to resonance stabilization but, moreover, the transition state makes a large vibrational contribution to the entropy. The internal mobility is enhanced on formation of the transition state since formation of the allenic C=C=C moiety requires that the resonant allyl π system be broken on going from reactant to transition state, as illustrated in Figure 3. The vibrational activation entropy for this β-scission is some $+15$ J mol^{-1} K^{-1} as compared to -9 J mol^{-1} K^{-1} for the vibrational activation entropy of the reference β-scission of the ethyl radical.

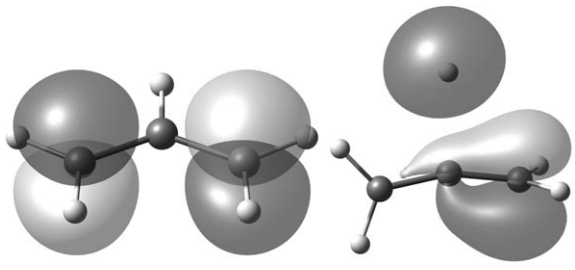

Figure 3. Allyl radical (left) and transition state (right) for β-scission of the allyl radical yielding allene, with HOMO depicted (95% contour).

2.4. Group-Additive Values

Group-additive values ΔGAV° were determined from the Arrhenius parameters of 34 reactions listed in Tables 3 and 4. All ΔGAV° were determined from a single reaction.

Table 5 lists the resulting group additive values for 300 and 1000 K. Group-additive values at 600 K can be found in Table S8 of the Supporting Information. The single-event Arrhenius parameters for the reference reaction are given in Table 6 for temperatures between 300 and 1300 K.

A closer look at the group additive values in Table 5 provides a clear view of the effect of substituents on C_1 and C_2 on the kinetics. Most $\Delta GAV^\circ(C_1)$ relate to stabilization of the product radical with respect to the reference reaction, and hence the group additive values for the activation energy of addition are negative, while those for β-scission are strongly positive. The β-scission activation energy increases up to 75 kJ mol^{-1} for the diallylic radical group $C_1(C_d)_2$ (group C_1-5). The substituents at C_1 have little effect on the pre-exponential factor for addition, as discussed previously. For β-scission, the ΔGAV° for pre-exponential factors are generally positive, partially compensating the effect of E_a on the kinetics.

The group additive values accounting for the influence of substitution at the attacked C_2 carbon atom $\Delta GAV^\circ(C_2)$ have a strong rate-decreasing effect on addition through a combination of a decrease in the pre-exponential factor and an increase in the activation energy. There are two exceptions: the C_{2t}-(H) and C_{2t}-(C_t) groups (resp. C_2-13 and C_2-16) have a large positive contribution to lg A. These ΔGAV° were determined from hydrogen addition to the linear molecules ethyne and buta-1,3-diyne discussed above. For β-scissions, the contributions of substituents on C_2 increase the rate coefficient. As discussed above, the substituents on C_2 stabilize the formed alkene more than the radical, and this leads to negative ΔGAV° for the β-scission activation energies. Contributions to lg A for β-scissions are generally slightly positive and add to the rate-

Table 5. Group-additive values ΔGAV° for the C_1 and C_2 carbon atoms (see Figure 1) for hydrogen addition Arrhenius parameters ($m^3 mol^{-1} s^{-1}$ for addition, s^{-1} for β-scission, and kJ mol^{-1} for E_a).

No.	Group[a]	300 K				1000 K			
		Addition		β-scission		Addition		β-scission	
		lg $\tilde{A}$	E_a	lg $\tilde{A}$	E_a	lg $\tilde{A}$	E_a	lg $\tilde{A}$	E_a
Reference reaction		7.010	10.4	12.012	156.3	7.726	18.5	12.580	162.4
C_1-1	C_1-(C)(H)	+0.017	−2.4	+0.154	−2.1	+0.019	−2.4	+0.224	−1.4
C_1-2	C_1-$(C)_2$	+0.068	−4.9	+0.268	−4.9	+0.072	−4.9	+0.452	−3.2
C_1-3	C_1-(C_d)(H)	−0.035	−7.1	+0.717	+40.9	−0.024	−7.0	+0.861	+42.2
C_1-4	C_1-(C_d)(C)	+0.002	−9.1	+0.152	+38.8	+0.023	−8.9	+0.303	+40.2
C_1-5	C_1-$(C_d)_2$	−0.043	−10.4	+0.062	+74.9	−0.022	−11.4	+0.273	+76.9
C_1-6	C_1-(C_t)(H)	−0.036	−5.5	+0.311	+36.0	−0.028	−5.4	+0.420	+37.0
C_1-7	C_1-(C_t)(C)	+0.013	−7.0	+0.096	+35.5	+0.022	−6.9	+0.244	+36.9
C_1-8	C_1-(C_t)(C_d)	−0.033	−9.7	+0.473	+62.1	−0.012	−9.5	+0.663	+63.9
C_1-9	C_1-$(C_t)_2$	−0.050	−8.3	−0.507	+62.5	−0.037	−8.2	−0.308	+64.5
C_1-10	C_1-(C_b)(H)	−0.593	+2.1	+0.492	+39.0	−0.595	+2.1	+0.642	+40.4
C_1-11	C_1-(C_b)(C)	−0.142	−0.3	−0.055	+34.1	−0.133	−0.3	+0.128	+35.9
C_1-12	$C_{1,allene}$-	−0.012	+1.0	+0.711	+8.0	−0.048	+0.6	+0.989	+10.7
C_1-13	$C_{1,allenell}$(C)-(H)	+0.050	−4.9	+0.035	+0.7	+0.071	−4.7	+0.018	+0.6
C_1-14	$C_{1,allenell}$-$(C)_2$	−0.141	−8.4	−0.598	−1.4	−0.165	−8.7	−0.662	−2.0
C_1-15	C_{1t}-(C)	−0.553	−2.0	+0.082	−1.1	−0.299	+0.8	+0.048	−1.5
C_1-16	C_{1t}-(C_d)	−0.811	−8.5	−0.068	+35.2	−0.547	−5.5	−0.225	+33.6
C_1-17	C_{1t}-(C_t)	−0.035	−7.3	−0.465	+27.5	−0.036	−7.3	−0.990	+25.4
C_2-1	C_2-(C)(H)	−0.188	+4.3	+0.481	−8.2	−0.217	+4.0	+0.475	−8.3
C_2-2	C_2-$(C)_2$	−0.426	+8.0	+0.412	−13.5	−0.493	+7.4	+0.370	−13.9
C_2-3	C_2-(C_d)(H)	−0.133	+6.4	+0.302	−21.3	−0.132	+6.4	+0.305	−21.3
C_2-4	C_2-(C_d)(C)	−0.306	+9.8	+0.200	−25.1	−0.323	+9.7	+0.164	−25.5
C_2-5	C_2-$(C_d)_2$	−0.196	+12.6	+0.032	−25.4	−0.196	+12.7	−0.005	−25.8
C_2-6	C_2-(C_t)(H)	−0.158	+7.5	+0.070	−15.6	−0.161	+7.6	+0.086	−15.4
C_2-7	C_2-(C_t)(C)	−0.341	+12.5	+0.262	−17.5	−0.366	+12.4	+0.226	−17.9
C_2-8	C_2-(C_t)(C_d)	−0.206	+14.8	+0.288	−29.7	−0.182	+15.1	+0.282	−29.7
C_2-9	C_2-$(C_t)_2$	−0.225	+17.5	+0.492	−23.3	−0.204	+17.8	+0.481	−23.4
C_2-10	C_2-(C_b)(H)	−0.653	+15.6	−0.306	−4.7	−0.663	+15.5	−0.300	−4.7
C_2-11	C_2-(C_b)(C)	−0.484	+15.3	−0.036	−9.3	−0.517	+15.1	−0.052	−9.5
C_2-12	$C_{2,allene}$	+0.054	+8.9	+1.695	+100.9	+0.014	+8.6	+1.938	+103.0
C_2-13	C_{2t}-(H)	+0.868	+6.7	+1.544	+9.7	+0.595	+3.7	+1.879	+12.8
C_2-14	C_{2t}-(C)	+0.058	+10.9	+1.484	−1.0	+0.015	+10.5	+1.755	+1.3
C_2-15	C_{2t}-(C_d)	+0.101	+11.4	+1.722	+11.4	+0.077	+11.2	+2.016	+14.0
C_2-16	C_{2t}-(C_t)	+0.783	+15.4	+1.370	+2.4	+0.523	+12.5	+1.700	+5.3

[a] Group notation: central atom-(ligands). C: sp_3 carbon atom, C_d: doubly bonded carbon atom , C_t: triply bonded carbon atom, C_B: carbon atom forming part of a benzene ring.

Table 6. Single-event Arrhenius parameters for the reference reaction H + ethene.

T	Addition		β-scission	
	$\lg \tilde{A}_{ref}$	$E_{a,ref}$	$\lg \tilde{A}_{ref}$	$E_{a,ref}$
[K]	[$m^3 mol^{-1} s^{-1}$]	[$kJ mol^{-1}$]	[s^{-1}]	[$kJ mol^{-1}$]
300	7.010	10.4	12.012	156.3
400	7.153	11.3	12.150	157.2
500	7.283	12.4	12.265	158.1
600	7.396	13.6	12.358	159.1
700	7.494	14.8	12.433	160.0
800	7.580	16.0	12.493	160.9
900	7.657	17.3	12.541	161.7
1000	7.726	18.5	12.580	162.4
1100	7.788	19.8	12.611	163.0
1200	7.845	21.0	12.637	163.6
1300	7.897	22.3	12.659	164.1

increasing character of the ΔGAV° for E_a. Exceptions to these general trends for the C_2 contributions to the β-scission rate coefficients are the reactions involving triple bonds and allene (groups C_2-12 to C_2-16), for which ΔGAV° is positive for E_a and strongly positive for lg A, up to ΔGAV°(lg A) = 2, due to the increase in mobility on transition state formation compared to the reference reaction.

As illustrated in Figure 4, the temperature dependence of ΔGAV° is limited in the range 300–1300 K. For addition reactions, the ΔGAV° vary by less than 1 $kJ mol^{-1}$ in the activation energy and 0.1 in the pre-exponential factor for all but four groups (Figure 4). For β-scission, the temperature dependence is somewhat larger but remains limited to 3 $kJ mol^{-1}$ in activation energies and 0.34 in pre-exponential factors. Compared to the temperature dependence of the actual Arrhenius parameter in this temperature range, that is, between +0.5 and +1.0 for lg A and +7 to +12 $kJ mol^{-1}$ for E_a, these values are small, that is, most of the temperature dependence of the kinetic parameters is indeed accounted for by $E_a(T)$ and lg $A(T)$ of the reference reaction. Larger temperature dependences for addition are observed for the ΔGAV° for the C_{1t}-(C), C_{1t}-(C_d), C_{2t}-(H), and C_{2t}-(C_t) groups, for which the ΔGAV° for E_a vary by about 4 $kJ mol^{-1}$ between 300 and 1300 K. The increased temperature dependence is again related to the linearity of the reactants ethyne and buta-1,3-diyne, from which the ΔGAV° were derived for the C_{2t}-(H) and C_{2t}-(C_t) groups, respectively. The temperature dependence of the additional vibration in the linear molecule ($C_p \approx R$) is larger than for the lost external rotational degree of freedom ($C_p = R/2$), which explains the decrease in ΔGAV° with increasing temperature. The ΔGAV° for the other two groups, C_{1t}-(C) and C_{1t}-(C_d), are derived from hydrogen additions to propyne and but-1-en-3-yne. These reactants are not linear, but since these reactions also involve the C_{2t}-(H) group, the ΔGAV° for the C_{1t}-(C) and C_{1t}-(C_d) groups have inverse temperature dependence and increase with temperature. In the temperature range of 1000 K however, a difference of 4 $kJ mol^{-1}$ can still be considered acceptable. In most applications the kinetics are required in a much narrower temperature range. Moreover, the positive correlation between the variation with temperature of both Arrhenius parameters limits the deviations in the rate coefficients to a factor of three for all groups, even if 300 K ΔGAV° are used at 1300 K and vice versa. When the four C_t groups are excluded, the deviations in the rate coefficient are even limited to a factor of two.

From the discussions above, it is clear that addition to triple and allenic bonds show different behavior to addition to double bonds. This different behavior is also reflected in the magnitude and temperature dependence of their group additive values. Although their inclusion in the same family of reactions is questionable, the differentiation between C_d and C_t carbon atoms made in the group additive method allows description of their kinetics. As such, the groups describing additions to triple bonds can be seen to form a subset including all groups centered on a C_t atom, and thus inclusion of addition to double and triple bonds in the same family of reactions and using the same reference reaction is enabled.

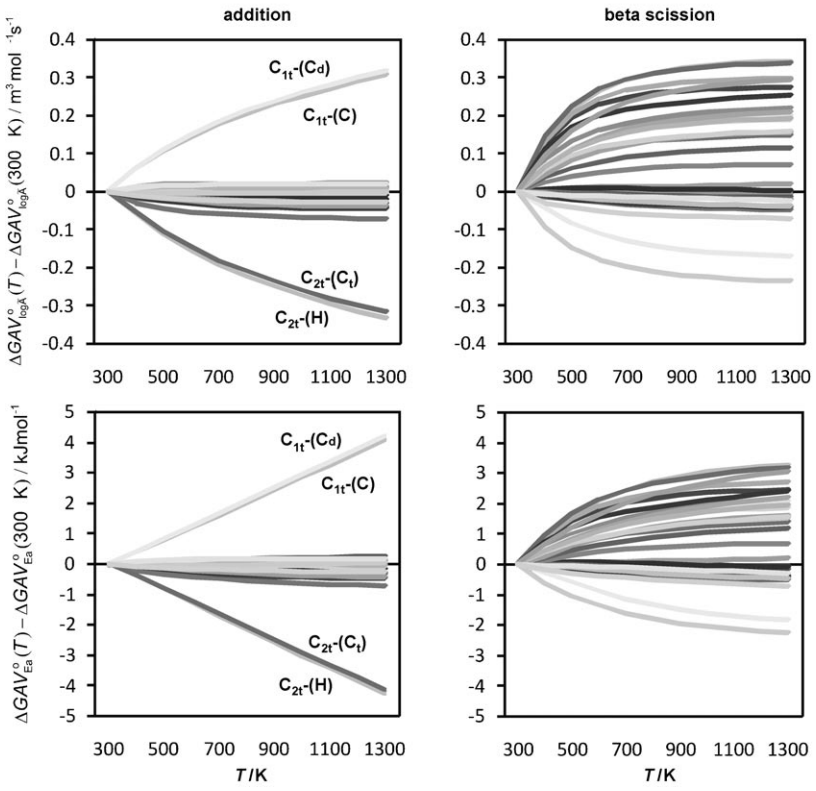

Figure 4. Temperature dependence of the group additive values relative to the ΔGAV° at 300 K.

2.5. Tunneling Correction

The ΔGAV° reported in Table 5 do not include contributions of quantum mechanical tunneling effects. However, an accurate description of the kinetics for the hydrogen addition/β-scission reactions requires inclusion of tunneling effects, since these are significant at temperatures below 400 K. In this section, an approach is presented to obtain tunneling corrections for reactions belonging to the hydrogen addition/β-scission family as function of the temperature and activation energy for the addition reaction, $\kappa[T,E_{a,add}(T)]$. This approach allows easy determination of tunneling corrections for all reactions to which the group additivity model presented here applies. Note that $E_{a,add}(T)$ pertains to the activation energy of addition that can be predicted by using the group additive values presented above, taken at the appropriate temperature.

Figure 5 presents the correlation between the Eckart tunneling coefficients and activation energies of addition for the reactions in Table 3 and 4. At 300 K, the tunneling coefficients

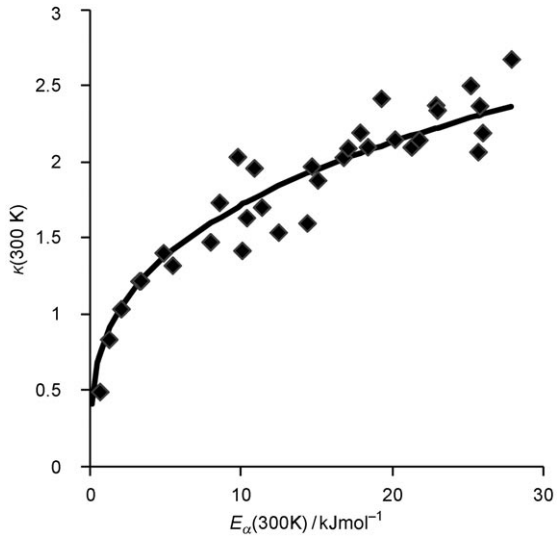

Figure 5. Tunneling coefficients versus activation energy at 300 K for the reactions of Tables 1 and 2 (◆) and the regression of Equation (10) (——).

range between 0.5 and 2.7. Because of the presence of reflection at low barriers, a power law provides the best description of the tunneling behavior. Equation (9) was obtained by regression of tunneling coefficients in the range 300–1000 K (see Table S9 of the Supporting Information) to the activation energies at the respective temperatures [Eq. (9)]:

$$\kappa(T, E_{a,add(T)}) = 0.84\left(E_{a,addition}\right)^{\frac{56}{T-120}} \quad (9)$$

where $E_{a,add}(T)$ has units of kilojoules per mole and T is in kelvin. The excellent agreement shown in Figure 5 yields a mean $\langle\rho\rangle$ of only 1.07 between the power-law-predicted and the Eckart tunneling coefficients at 300 K. The largest deviation is an acceptable factor of 1.2. At higher temperatures, the average deviations decrease. The remaining deviations are functions of the imaginary frequency, which is, however, not accessible during group additivity predictions. Correction for tunneling contributions is important only at temperatures up to 400 K. For temperatures of 500 K and higher, tunneling makes only a marginal contribution and can thus be neglected.

An alternative correlation expressing the tunneling coefficient as function of the tunneling coefficient of the reference reaction, in line with the approach of Truong et al. for hydrogen abstractions, as discussed in the Computational Methods section,[26,60,66,67] is given in the Supporting Information.

2.6. Application and Validation of the Method

In this section, first the application of the group additive method for the calculation of the Arrhenius parameters is illustrated. Next, the obtained group additive model is validated by comparing group additive predictions to 1) 11 ab-initio-calculated rate coefficients for addition to various types of unsaturated hydrocarbons (see Tables 7 and 8) and 2) seven experimental rate coefficients (see Table 9).

To obtain the pre-exponential factor and activation energy for hydrogen addition to *trans*-2-butene (reaction 1a in Table 7), for instance, the required ΔGAV° are those for the C_1-(C)(H) and C_2-(C)(H) groups pertaining to the methyl substituents on the C_1 and the C_2 carbon atoms. At 1000 K, the activation energy for this addition can be written as Equation (10):

$$\begin{aligned} E_a(1000\ \mathrm{K}) &= E_{a,ref} + \Delta GAV^{\circ}_{E_a}[C_1\text{-}(C)(H)] + \Delta GAV^{\circ}_{E_a}[C_2\text{-}(C)(H)] \\ &= 18.5 - 2.4 + 4.0 = 20.1\ \mathrm{kJ\,mol^{-1}} \end{aligned} \quad (10)$$

while the ab-initio-calculated activation energy is 18.9 kJ mol^{-1}, an overestimation of only 1.2 kJ mol^{-1}. Similarly, at 1000 K, the β-scission activation energy can be calculated to be 152.7 kJ mol^{-1}, which is only 0.6 kJ mol^{-1} lower than the ab-initio-calculated activation energy. The calculation of the pre-exponential factor requires the number of single events to be determined. For the reactant *trans*-2-butene, the external symmetry number is 2 and the internal symmetry number is $3^2=9$. For hydrogen $\sigma=1$. The transition state has no external symmetry but still has ninefold internal symmetry and exhibits molecular chirality, that is, $n_{opt}=2$. With these values, the number of single events for addition can be written as Equation (11):

$$n_e = \frac{n_{opt,\ddagger}}{\prod_j n_{opt,j}} \frac{\prod_j \sigma_j}{\sigma_{\ddagger}} = \frac{2}{(1\cdot 1)} \frac{(1\cdot 1)(2\cdot 9)}{1\cdot 9} = 4 \quad (11)$$

The pre-exponential factor can then be calculated as Equation (12):

$$\begin{aligned} &\lg[A(1000\ \mathrm{K})/\mathrm{m^3\,mol^{-1}\,s^{-1}}] \\ &= \lg \tilde{A}_{ref} + \Delta GAV^{\circ}_{\lg \tilde{A}}[C_1\text{-}(C)(H)] + \Delta GAV^{\circ}_{\lg \tilde{A}}[C_2\text{-}(C)(H)] + \lg n_e \\ &= 7.726 + 0.019 - 0.217 + \lg 4 = 8.130 \end{aligned} \quad (12)$$

which agrees very well with the ab-initio-calculated lg(*A*/

$m^3\,mol^{-1}\,s^{-1}$) of 8.158. For the reverse reaction, with a number of single events of 2, $\log(A/m^3\,mol^{-1}\,s^{-1})$ amounts to 13.580, as determined by group additivity, which is only 0.072 off of the ab initio value. At 1000 K, tunneling corrections can be neglected, and rate coefficients of $1.2\times10^7\ m^3\,mol^{-1}\,s^{-1}$ for addition and $4.0\times10^5\ s^{-1}$ for β-scission result, which are both within 30% of the respective ab-initio-calculated rate coefficients of $1.5\times10^7\ m^3\,mol^{-1}\,s^{-1}$ and $3.1\times10^5\ s^{-1}$.

Using these values, the rate coefficient at 300 K is found as Equation (15):

$$k(300\text{K}) = 1.83 \times 10^{7.441}\exp\left(-\frac{12.3\text{kJ mol}^{-1}}{RT}\right) = 3.6 \times 10^5\text{m}^3\,\text{mol}^{-1}\,\text{s}^{-1} \quad (15)$$

which is within 40% of the ab-initio-determined (tunneling-corrected) value of $5.8\ 10^5\ m^3\,mol^{-1}\,s^{-1}$.

Table 7. Group-additive model validation: comparison of group additive prediction with ab initio calculation for the tunneling coefficients, pre-exponential factors, and activation energies of addition (a) and β-scission (β) at 1000 K (tunneling contributions are neglected).

No.	Reaction	κ/κ_{Al}	300 K $\frac{A_{GA}}{A_{Al}}$	300 K $E_{a,GA}-E_{a,Al}$	1000 K $\frac{A_{GA}}{A_{Al}}$	1000 K $E_{a,GA}-E_{a,Al}$
1a	H + ⇄ 	1.01	0.92	+1.1	0.94	+1.2
1β			1.24	−0.5	1.18	−0.6
2a	H +  ⇄ 	1.01	0.95	+1.0	0.97	+1.1
2β			0.78	−5.7	0.76	−5.8
3a	H +  ⇄ 	1.01	1.21	+0.8	1.20	+0.7
3β			1.35	−0.9	1.36	−0.8
4a	H +  ⇄	1.05	1.25	−0.3	1.27	−0.2
4β			1.27	−0.7	1.29	−0.6
5a	H +  ⇄ 	1.12	4.32	+5.3	4.44	+5.4
5β			0.93	−12.5	0.88	−12.6
6a	H +  ⇄ 	1.14	1.15	+3.7	1.16	+3.6
6β			0.66	−0.1	0.63	−0.3
7a	H +  ⇄ 	0.93	2.84	+1.3	2.72	+1.1
7β			1.36	−1.4	1.44	−1.1
8a	H + ⇄ 	0.91	1.01	+0.6	1.05	+0.7
8β			1.37	+1.3	1.32	+1.1
9a	H + 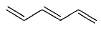 ⇄ 	0.90	0.89	−0.7	0.91	−0.7
9β			1.35	+2.4	1.31	+2.3
10a	H +  ⇄ 	1.08	2.42	+1.2	2.43	+1.2
10β			0.90	+3.1	0.90	+3.1
11a	H +  ⇄ 	0.86	1.22	−0.1	1.26	+0.1
11β			4.72	+6.5	5.22	+6.8

To obtain the kinetic parameters for this same addition at 300 K, the Arrhenius parameters for the reference reaction and the ΔGAV° at 300 K are used [Eq. (13)]:

$$E_a(300\text{ K}) = 10.4-2.4+4.3 = 12.3\text{ kJ mol}^{-1}$$
$$\lg A(300\text{ K}) = 7.010+0.017-0.188+\lg 4 = 7.441\text{ m}^3\,\text{mol}^{-1}\,\text{s}^{-1} \quad (13)$$

At 300 K tunneling correction is relevant and the tunneling coefficient $\kappa[T,E_{a,add}(T)]$ can be obtained as Equation (14):

$$\kappa(T,E_a) = 0.84\left(E_{a,\text{addition}}\right)^{\frac{56}{T-120}} = 0.84(12.3\text{ kJ mol}^{-1})^{\frac{56}{300\text{ K}-120}} = 1.83 \quad (14)$$

2.6.1. Ab Initio Validation

To validate the group additive method, the group-additive-predicted rate coefficients are compared to ab-initio-calculated rate coefficients for 11 hydrogen additions (see Tables 7 and 8) to unsaturated hydrocarbons ranging from butenes to strongly resonance-stabilized species such as 1,3,5-hexatriene and to allenic and triple bonds. The test reactions also include species for which deviation from the truncated group additive model is expected such as addition to 2,3-dimethylbut-2-ene, which suffers greatly from steric effects. Differences between ab-initio-calculated and group-additive-predicted Arrhenius parameters and tunneling coefficients can be found in Table 7 while differences in rate coefficients and equilibrium coefficients are presented in Table 8. The actual calculated and predicted values, the number of single events and the parameters characterizing the transition state are given in Tables S10–S12 of the Supporting Information. The group additive predictions use the ΔGAV° at the indicated temperature.

The tunneling coefficients at 300 K are predicted excellently by Equation (9), the largest deviations being 14%. The ratio between the predicted and ab initio pre-exponential factor is between 0.6 and 5 at 300 K; the largest deviations are observed for reactions 5 and 11 in Table 7. For activation energies, the mean absolute deviation between prediction and ab initio calculation amounts to 2.3 $kJ\,mol^{-1}$, with deviations ranging between −12.5 and 6.5 $kJ\,mol^{-1}$ (for reactions 5β and 11β). The deviations at 1000 K are similar to those at 300 K.

Reaction 5a, hydrogen addition to 2,3-dimethylbut-2-ene, which has deliberately been included since the strong steric effects present in this reaction will bias the group additive prediction, indeed shows the largest deviation in the activation energy. In the reactant alkene, a double-*cis* interaction is pres-

Table 8. Group additive validation: comparison of group additive (GA) prediction with ab initio (AI) calculation for the rate coefficients of addition (a) and β-scission (β), and equilibrium coefficients (1000 K tunneling contributions are neglected).

No.	Reaction	300 K k_{AI}	300 K $\frac{k_{GA,x}}{k_{AI}}$	300 K $\frac{K_{GA}^{eq}}{K_{AI}^{eq}}$	1000 K k_{AI}	1000 K $\frac{k_{GA,x}}{k_{AI}}$	1000 K $\frac{K_{GA}^{eq}}{K_{AI}^{eq}}$
1a	H + ⇄ 	5.8×10^{5}	0.63	0.38	1.5×10^{7}	0.82	0.64
1β		3.7×10^{-13}	1.66		3.1×10^{5}	1.28	
2a	H +  ⇄ 	5.3×10^{5}	0.68	0.08	1.4×10^{7}	0.86	0.57
2β		7.2×10^{-14}	8.53		2.6×10^{5}	1.52	
3a	H +  ⇄ 	7.6×10^{4}	0.93	0.46	3.9×10^{6}	1.11	0.73
3β		2.0×10^{-13}	2.02		2.7×10^{5}	1.51	
4a	H +  ⇄	9.0×10^{5}	1.53	0.82	1.2×10^{7}	1.31	0.94
4β		1.1×10^{-14}	1.87		1.1×10^{5}	1.39	
5a	H +  ⇄ 	2.6×10^{5}	0.59	0.004	2.8×10^{6}	2.33	0.58
5β		1.1×10^{-13}	162.98		3.2×10^{5}	4.02	
6a	H +  ⇄ 	1.2×10^{6}	0.31	0.37	1.6×10^{7}	0.75	1.16
6β		1.5×10^{-12}	0.83		1.2×10^{6}	0.65	
7a	H +  ⇄ 	5.8×10^{3}	1.73	0.71	6.4×10^{5}	2.39	1.45
7β		6.2×10^{-13}	2.43		1.9×10^{5}	1.65	
8a	H +  ⇄ 	1.2×10^{6}	0.77	0.95	9.8×10^{6}	0.97	0.84
8β		7.8×10^{-20}	0.81		7.9×10^{3}	1.16	
9a	H + 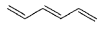 ⇄ 	8.5×10^{5}	1.14	2.27	1.7×10^{7}	0.99	1.00
9β		1.7×10^{-17}	0.50		3.0×10^{4}	1.00	
10a	H +  ⇄ 	4.4×10^{5}	1.70	5.42	9.1×10^{6}	2.10	3.38
10β		1.5×10^{-15}	0.31		1.1×10^{5}	0.62	
11a	H +  ⇄ 	1.0×10^{6}	1.18	3.55	1.3×10^{7}	1.25	0.54
11β		2.8×10^{-21}	0.33		1.8×10^{3}	2.30	
ρ(addition)			1.6			1.5	
ρ(β-scission)			17.3			1.7	
ρ(β-scission), excluding reaction 5			2.7			1.5	

ent, as illustrated in Figure 6. In the transition state, this *cis* strain is partially released due to the formation of the sp^3 center. As the truncated group additive method contains only primary contributions, the partial release of the *cis* strain in going from the alkene to the transition state is not accounted for, and this results in overestimation of the activation energy of the forward addition by 5.3 kJ mol^{-1}. For the reverse β-scission of the 2,3-dimethylbut-2-yl radical, an increased steric interaction is caused by the developing *cis* interaction in the transition state for formation of 2,3-dimethylbut-2-ene, leading to underestimation of the activation energy by 12.5 kJ mol^{-1}. In the truncated group additive method, the groups centered on the C_1 and C_2 carbon atoms are considered independent of each other. As a consequence, the mutual strain caused by the simultaneous presence of substituents on C_1 and C_2 cannot be accounted for by the truncated group additive method, as it does not include the tertiary contributions that are required to properly account for this effect. For this β-scission, the neglected mutual strain is larger in the transition state than in the reactant radical, where *gauche* interactions but no *cis* interactions are present. It can be shown quantitatively that the deviation in activation energy for this β-scission is caused by the *cis* interaction. The double-*cis* interaction present in 2,3-dimethylbutene has a contribution of 18.3 kJ mol^{-1} to the standard enthalpy of formation,[72] while the steric interaction of the two radical *gauche* interactions (type 1) in the product radical involves a *gauche* correction of 5.4 kJ mol^{-1}.[72] As the transition state for β-scission is very late, it can be assumed that the *cis* interaction is almost entirely developed in the transition state. Therefore, the neglected steric effect on the activation energy can be estimated to be about $18.3-5.4=12.9$ kJ mol^{-1}, which corresponds very well with the observed difference of 12.5 kJ mol^{-1} between group additive and ab initio activation energy. The same reasoning holds for β-scission of the but-2-yl radical forming *cis*-2-butene (reaction 2β). The activation energy is underpredicted by 5.7 kJ mol^{-1}, in very good agreement with the *cis* contribution to the standard enthalpy of formation of 5.9 kJ mol^{-1}.[72]

For all reactions, except those with strong steric interactions in the reactants (reactions 2β and 5β, see Table 8), the group-additive-predicted rate coefficients at 300 K are within a factor 3.5 of the ab-initio-predicted value. As discussed above, most troublesome is reaction 5β, for which the deviation of 12 kJ mol^{-1} in the β-scission activation energy causes the rate to be underestimated by a factor of 160 at 300 K. The addition rate coefficient for reaction 5a remains within a factor of 2. The second largest deviation is the overprediction by a factor of 8 for the β-scission of the but-2-yl radical (reaction 2), again caused by a *cis* interaction in the transition state. A parity plot of the group additive rate coefficients versus the ab-initio-calculated values is given in Figure 7. The mean factors of deviation $\langle\rho\rangle$ are 1.6 for addition and, due to the large deviation for reaction 5β, 17 for β-scission. On removing this outlier, the $\langle\rho\rangle$ value for β-scission drops to 2.7.

At 1000 K, the largest deviation in the rate coefficient is reduced to a factor of 4 for β-scission of the 2,3-dimethylbut-2-yl radical (reaction 5β). For all other reactions, the deviations are smaller than a factor 2.5; for 75% of the reactions they are even smaller than a factor 1.5, which can be considered an excellent agreement between prediction and ab initio calculation. The averaged mean factors of deviation $\langle\rho\rangle$ are 1.5 for addition and 1.7 for β-scission.

Table 9. Group-additive model validation: comparison of group additive predictions (including tunneling correction) with experimental values on the basis of ρ factors as defined in Equation (3), averaged out per reaction.

No.	Reaction	$\langle\rho\rangle$(addition)			$\langle\rho\rangle$(β-scission)		
		300 K	600 K	1000 K	300 K	600 K	1000 K
1	H +  ⇄ 	1.7			1.3	1.3	
2	H +  ⇄ 	1.5			1.3	2.3	1.8
3	H +  ⇄ 	1.3	1.4	2.0	1.1	1.8	1.8
4	H +  ⇄ 	1.7			8.2	1.3	1.1
5	H +  ⇄ 	4.9					
6	H +  ⇄ 	5.5					
7	H +  ⇄ 	1.5					
		$\langle\rho\rangle$	2.6	1.4	2.0	3.0	1.7	1.6
		$\langle\rho\rangle_{mean}$	2.0					

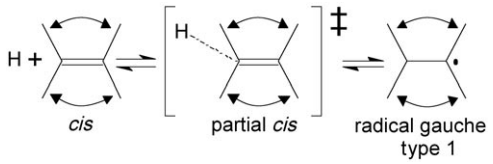

Figure 6. Reactant, transition state, and product for hydrogen addition to 2,3-dimethylbut-2-ene, indicating the non-nearest-neighbor interactions neglected by the group additive method.

From these results, it can be concluded that the truncated group additive method yields accurate predictions provided that no strong steric effects influence the kinetics. This is due to the neglect of tertiary contributions in the truncated group additive model which is restricted to primary effects, i.e., to the groups centered on the C_1 and C_2 atoms. These tertiary contributions, originating from non-nearest-neighbor interactions, are already difficult to model for thermodynamics, and modeling these interactions for kinetics is expected to be even more troublesome.[72] The neglect of tertiary contributions, however, does not have significant effects on the accuracy of the rate coefficients for addition. Therefore, for reactions with severe steric effects, it is suggested to calculate the β-scission rate coefficient from the addition rate coefficient and the thermodynamic equilibrium coefficient. And since accurate equilibrium coefficients are of primary importance for use in reaction networks, best results will be obtained by calculating the β-scission rate coefficient from the addition rate and the equilibrium coefficient for all reactions, with explicit implementation of thermodynamic consistency. The thermodynamic equilibrium can be calculated using thermochemical group additivity, which predicts equilibrium coefficients more reliably, typically within a factor of two.[73]

Based on the reactions of Table 7, the group additive method outperforms models such as Evans–Polanyi correlations.[15,16] Applying an Evans–Polanyi relation obtained from the reactions in Tables 3 and 4 for prediction of the 300 K activation energies of Table 7, an average overestimation of the ab initio activation energies of 4.3 kJ mol^{-1} is found, compared to an overestimation by 1.3 kJ mol^{-1} for the group additive method (see Figure S5 and S6 in the Supporting Information). Group additivity clearly improves the agreement with the ab initio activation energy, and the method is moreover capable of predicting pre-exponential factors in contrast to the Evans–Polanyi method.

2.6.2. Experimental Validation

In this section, the group-additive-predicted rate coefficients are compared to experimentally determined rate coefficients at 300, 600, and 1000 K (see Table 9). The seven reactions all involve hydrogen addition/β-scission data available in the NIST Chemical Kinetics Database[69] that have not been used previously for the validation of the computational method. From the 16 rate coefficients for addition in the 300 K category, 10 were determined at 296, 298, or 303 K. For the sake of conciseness, we included these rate coefficients in the 300 K category.

In Table 9, the ρ values averaged per reaction are given. The actual experimental rate coefficients are given in Table S13 of the Supporting Information, and the individual deviation ratios and ρ values in Tables S14–S15. For four of the seven reactions in Table 9, the ρ values are smaller than a factor of three at all temperatures. At 600 and 1000 K, all deviations are smaller than a factor of three, while the larger deviations observed at 300 K indicate that the deviations are most possibly related to differences in the activation energy. The largest deviation occurs for the β-scission of the but-2-yl radical forming 1-butene (reaction 4 in Table 9), with a $\langle\rho\rangle$ value of 8.2 at 300 K. Averaged over all reactions and over the temperature range 300–1000 K, a mean factor of deviation $\langle\rho\rangle$ of 2.0 is found, which indicates excellent agreement between the group additive method and the experimental rate coefficients for this family of reactions. This mean factor of deviation of two mainly originates from the mean factor of deviation between the CBS-QB3 calculated values and experiment, for which a $\langle\rho\rangle$ value of 1.9 was obtained, as discussed above.

3. Conclusions

This study provides a group additive model for the kinetics of hydrogen addition. The applied model is an extension of the previously published group additive method for addition of carbon-centered radicals,[29] and allows the prediction of hydrogen addition and β-scission rate coefficients for a wide range of unsaturated hydrocarbons.

The rate coefficients are calculated by means of conventional transition-state theory based on ab initio CBS-QB3 calcula-

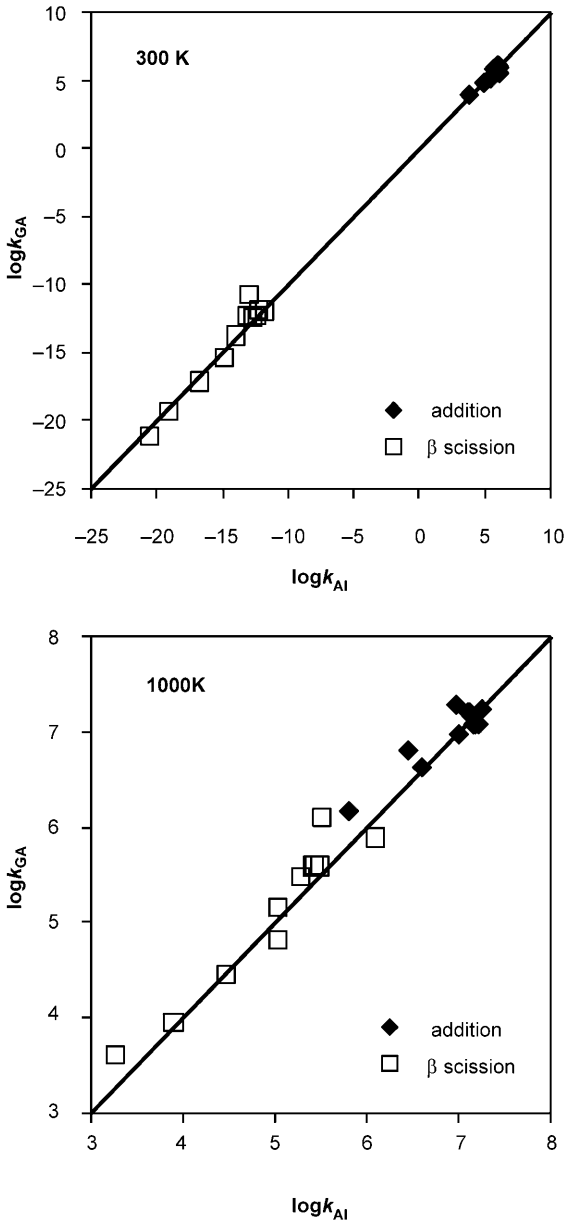

Figure 7. Parity plot of the group-additive-predicted rate coefficients [$m^3 mol^{-1} s^{-1}$] versus the ab-initio-calculated rate coefficients for the reactions from Table 8.

tions, with Eckart tunneling corrections. This computational approach is validated with experimental data for a set of seven reactions, for which a mean factor of deviation of only 1.9 is found in the temperature range 300–1000 K.

From CBS-QB3 calculated Arrhenius parameters, a set of group additive values ΔGAV° for activation energies and pre-exponential factors was derived. The temperature dependence of these ΔGAV° is, except for four C_{1t}-centered groups, very low. Therefore, a set of ΔGAV° at a single temperature is sufficient to describe the kinetics, even for a process with wide temperature ranges. Tunneling, which is significant at 400 K and below, is modeled separately, since it cannot be incorporated into the additivity method. A power-law correlation between the tunneling coefficients and the activation energy for addition, the latter being predicted by group additivity, successfully describes the tunneling coefficients.

The obtained group additive model was validated by comparing predicted rate coefficients with ab-initio-calculated rates for 11 reactions. The rate coefficients are predicted well, except for reactions with strong steric effects, such as addition to 2,3-dimethylbut-2-ene. For additions, the mean factor of deviation between prediction and ab initio rate coefficient is 1.6 at 300 K and 1.5 at 1000 K. For β-scissions, the agreement is less good, since steric effects contribute more to the rate, which also leads to inaccurate predictions of the equilibrium coefficients. Therefore, calculation of the β-scission rate coefficients from the addition rates and the thermodynamic equilibrium is advised.

Further comparison of predicted with experimental data for seven reactions in the range 300–1000 K yielded a mean factor of deviation of 2.0, which is of the same magnitude as the performance of the CBS-QB3 method in comparison with experimental rate coefficients. Hence, the presented group additive method can be reliably applied to predict rate coefficients for addition of hydrogen radicals with a reasonable accuracy over the whole temperature range 300–1000 K.

Acknowledgements

M.K.S. held a Ph.D. grant of the Institute for the Promotion of Innovation through Science and Technology in Flanders (IWT-Vlaanderen) and is grateful for financial support from the Fund for Scientific Research-Flanders (F.W.O.-Vlaanderen)

Keywords: ab initio calculations · gas-phase reactions · group additivity methods · kinetics · radical reactions

[1] H. Z. R. Zhang, E. G. Eddings, A. F. Sarofim, *Energy Fuels* **2007**, *21*, 677–685.
[2] E. Ranzi, M. Dente, S. Plerucci, G. Biardi, *Ind. Eng. Chem. Fund.* **1983**, *22*, 132–139.
[3] P. J. Clymans, G. F. Froment, *Comput. Chem. Eng.* **1984**, *8*, 137–142.
[4] L. P. Hillewaert, J. L. Dierickx, G. F. Froment, *AIChE J.* **1988**, *34*, 17–24.
[5] L. J. Broadbelt, S. M. Stark, M. T. Klein, *Comput. Chem. Eng.* **1996**, *20*, 113–129.
[6] F. Battin-Leclerc, P. A. Glaude, V. Warth, R. Fournet, G. Scacchi, G. M. Côme, *Chem. Eng. Sci.* **2000**, *55*, 2883–2893.
[7] S. Wauters, G. B. Marin, *Chem. Eng. J.* **2001**, *82*, 267–279.
[8] W. H. Green, P. I. Barton, B. Bhattacharjee, D. M. Matheu, D. A. Schwer, J. Song, R. Sumathi, H. H. Carstensen, A. M. Dean, J. M. Grenda, *Ind. Eng. Chem. Res.* **2001**, *40*, 5362–5370.
[9] M. Dente, G. Bozzano, T. Faravelli, A. Marongiu, S. Pierucci, E. Ranzi, *Adv. Chem. Eng.* **2007**, *32*, 51–166.
[10] W. H. Green Jr. , *Adv. Chem. Eng.* **2007**, *32*, 1–50.
[11] S. Pierucci, E. Ranzi, *Comput. Chem. Eng.* **2008**, *32*, 805–826.
[12] K. M. Van Geem, M. F. Reyniers, G. B. Marin, J. Song, D. M. Matheu, W. H. Green, *AIChE J.* **2006**, *52*, 718–730.
[13] J. Zádor, I. G. Zsély, T. Turányi, M. Ratto, S. Tarantola, A. Saltelli, *J. Phys. Chem. A* **2005**, *109*, 9795–9807.
[14] R. G. Susnow, A. M. Dean, W. H. Green, P. Peczak, L. J. Broadbelt, *J. Phys. Chem. A* **1997**, *101*, 3731–3740.
[15] M. G. Evans, M. Polanyi, *Proc. R. Soc. A—Math. Phys. Eng. Sci.* **1936**, *154*, 1333–1360.
[16] M. G. Evans, M. Polanyi, *Trans. Faraday Soc.* **1938**, *34*, 11–29.
[17] P. Blowers, R. Masel, *AIChE J.* **2000**, *46*, 2041–2052.
[18] S. W. Benson, J. H. Buss, *J. Chem. Phys.* **1958**, *29*, 546–561.

[19] S. W. Benson, *Thermochemical Kinetics*, 1st ed., Wiley, New York, **1968**.
[20] P. A. Willems, G. F. Froment, *Ind. Eng. Chem. Res.* **1988**, *27*, 1959 – 1966.
[21] P. A. Willems, G. F. Froment, *Ind. Eng. Chem. Res.* **1988**, *27*, 1966 – 1971.
[22] R. Sumathi, H. H. Carstensen, W. H. Green, *J. Phys. Chem. A* **2001**, *105*, 6910 – 6925.
[23] R. Sumathi, H. H. Carstensen, W. H. Green, *J. Phys. Chem. A* **2001**, *105*, 8969 – 8984.
[24] R. Sumathi, H. H. Carstensen, W. H. Green, *J. Phys. Chem. A* **2002**, *106*, 5474 – 5489.
[25] T. N. Truong, *J. Chem. Phys.* **2000**, *113*, 4957 – 4964.
[26] S. W. Zhang, T. N. Truong, *J. Phys. Chem. A* **2003**, *107*, 1138 – 1147.
[27] M. Saeys, M. F. Reyniers, G. B. Marin, V. Van Speybroeck, M. Waroquier, *AIChE J.* **2004**, *50*, 426 – 444.
[28] M. Saeys, M. F. Reyniers, V. Van Speybroeck, M. Waroquier, G. B. Marin, *ChemPhysChem* **2006**, *7*, 188 – 199.
[29] M. K. Sabbe, M. F. Reyniers, V. Van Speybroeck, M. Waroquier, G. B. Marin, *ChemPhysChem* **2008**, *9*, 124 – 140.
[30] D. L. Baulch, C. J. Cobos, R. A. Cox, C. Esser, P. Frank, T. Just, J. A. Kerr, M. J. Pilling, J. Troe, R. W. Walker, J. Warnatz, *J. Phys. Chem. Ref. Data* **1992**, *21*, 411 – 734.
[31] D. L. Baulch, C. T. Bowman, C. J. Cobos, R. A. Cox, T. Just, J. A. Kerr, M. J. Pilling, D. Stocker, J. Troe, W. Tsang, R. W. Walker, J. Warnatz, *J. Phys. Chem. Ref. Data* **2005**, *34*, 757 – 1397.
[32] W. Tsang, R. F. Hampson, *J. Phys. Chem. Ref. Data* **1986**, *15*, 1087 – 1279.
[33] W. Tsang, *J. Phys. Chem. Ref. Data* **1988**, *17*, 887 – 952.
[34] W. Tsang, *J. Phys. Chem. Ref. Data* **1990**, *19*, 1 – 68.
[35] W. Tsang, *J. Phys. Chem. Ref. Data* **1991**, *20*, 221 – 273.
[36] H. J. Curran, *Int. J. Chem. Kinet.* **2006**, *38*, 250 – 275.
[37] T. Gilbert, T. L. Grebner, I. Fischer, P. Chen, *J. Chem. Phys.* **1999**, *110*, 5485 – 5488.
[38] Y. Feng, J. T. Niiranen, A. Bencsura, V. D. Knyazev, D. Gutman, W. Tsang, *J. Phys. Chem.* **1993**, *97*, 871 – 880.
[39] B. S. Jursic, *J. Chem. Soc. Perkin Trans. 2* **1997**, 637 – 641.
[40] M. T. Nguyen, S. Creve, L. G. Vanquickenborne, *J. Phys. Chem.* **1996**, *100*, 18422 – 18425.
[41] H. Fischer, L. Radom, *Angew. Chem.* **2001**, *113*, 1380 – 1414; *Angew. Chem. Int. Ed.* **2001**, *40*, 1340 – 1371.
[42] S. S. Shaik, E. Canadell, *J. Am. Chem. Soc.* **1990**, *112*, 1446 – 1452.
[43] J. S. Clarke, H. A. Rypkema, J. H. Kroll, N. M. Donahue, J. G. Anderson, *J. Phys. Chem. A* **2000**, *104*, 4458 – 4468.
[44] J. A. Miller, S. J. Klippenstein, *Phys. Chem. Chem. Phys.* **2004**, *6*, 1192 – 1202.
[45] S. J. Klippenstein, J. A. Miller, *J. Phys. Chem. A* **2005**, *109*, 4285 – 4295.
[46] J. Villà, A. González-Lafont, J. M. Lluch, D. G. Truhlar, *J. Am. Chem. Soc.* **1998**, *120*, 5559 – 5567.
[47] J. Villà, J. C. Corchado, A. González-Lafont, J. M. Lluch, D. G. Truhlar, *J. Am. Chem. Soc.* **1998**, *120*, 12 141 – 12 142.
[48] J. Villà, J. C. Corchado, A. González-Lafont, J. M. Lluch, D. G. Truhlar, *J. Phys. Chem. A* **1999**, *103*, 5061 – 5074.
[49] E. T. Denisov, *Russ. Chem. Bull.* **2004**, *53*, 1602 – 1608.
[50] E. T. Denisov, A. F. Shestakov, N. S. Emel'yanova, *Kinet. Catal.* **2006**, *47*, 647 – 661.
[51] E. T. Denisov, *Kinet. Catal.l* **2008**, *49*, 313 – 324.
[52] J. A. Montgomery, M. J. Frisch, J. W. Ochterski, G. A. Petersson, *J. Chem. Phys.* **1999**, *110*, 2822 – 2827.
[53] M. K. Sabbe, A. G. Vandeputte, Ab initio group additivity method for the calculation of kinetic parameters for hydrogen abstractions, unpublished work, **2008**.
[54] M. Saeys, M. F. Reyniers, G. B. Marin, V. Van Speybroeck, M. Waroquier, *J. Phys. Chem. A* **2003**, *107*, 9147 – 9159.
[55] *Gaussian 03 (Revision B.03)*, M. J. Frisch, G. W. Trucks, H. B. Schlegel, G. E. Scuseria, M. A. Robb, J. R. Cheeseman, J. A. Montgomery, T. Vreven, K. N. Kudin, J. C. Burant, J. M. Millam, S. S. Iyengar, J. Tomasi, V. Barone, B. Mennucci, M. Cossi, G. Scalmani, N. Rega, G. A. Petersson, H. Nakatsuji, M. Hada, M. Ehara, K. Toyota, R. Fukuda, J. Hasegawa, M. Ishida, T. Nakajima, Y. Honda, O. Kitao, H. Nakai, M. Klene, X. Li, J. E. Knox, H. P. Hratchian, J. B. Cross, V. Bakken, C. Adamo, J. Jaramillo, R. Gomperts, R. E. Stratmann, O. Yazyev, A. J. Austin, R. Cammi, C. Pomelli, J. W. Ochterski, P. Y. Ayala, K. Morokuma, G. A. Voth, P. Salvador, J. J. Dannenberg, V. G. Zakrzewski, S. Dapprich, A. D. Daniels, M. C. Strain, O. Farkas, D. K. Malick, A. D. Rabuck, K. Raghavachari, J. B. Foresman, J. V. Ortiz, Q. Cui, A. G. Baboul, S. Clifford, J. Cioslowski, B. B. Stefanov, G. Liu, A. Liashenko, P. Piskorz, I. Komaromi, R. L. Martin, D. J. Fox, T. Keith, M. A. Al-Laham, C. Y. Peng, A. Nanayakkara, M. Challacombe, P. M. W. Gill, B. Johnson, W. Chen, M. W. Wong, C. Gonzalez, J. A. Pople >, Gaussian, Inc., Wallingford, CT, **2004**.
[56] D. K. Malick, G. A. Petersson, J. A. Montgomery, *J. Chem. Phys.* **1998**, *108*, 5704 – 5713.
[57] K. J. Laidler, *Chemical Kinetics*, 3rd ed., Harper Collins, New York, **1987**.
[58] C. Eckart, *Phys. Rev.* **1930**, *35*, 1303 – 1309.
[59] T. N. Truong, W. T. Duncan, M. Tirtowidjojo, *Phys. Chem. Chem. Phys.* **1999**, *1*, 1061 – 1065.
[60] N. Kungwan, T. N. Truong, *J. Phys. Chem. A* **2005**, *109*, 7742 – 7750.
[61] A. G. Vandeputte, M. K. Sabbe, M. F. Reyniers, V. Van Speybroeck, M. Waroquier, G. B. Marin, *J. Phys. Chem. A* **2007**, *111*, 11771 – 11786.
[62] M. K. Sabbe, A. G. Vandeputte, M. F. Reyniers, V. Van Speybroeck, M. Waroquier, G. B. Marin, *J. Phys. Chem. A* **2007**, *111*, 8416 – 8428.
[63] E. L. I. Pollak, P. Pechukas, *J. Am. Chem. Soc.* **1978**, *100*, 2984 – 2991.
[64] D. R. Coulson, *J. Am. Chem. Soc.* **1978**, *100*, 2992 – 2996.
[65] M. A. Baltanas, K. K. Vanraemdonck, G. F. Froment, S. R. Mohedas, *Ind. Eng. Chem. Res.* **1989**, *28*, 899 – 910.
[66] L. K. Huynh, S. Panasewicz, A. Ratkiewicz, T. N. Truong, *J. Phys. Chem. A* **2007**, *111*, 2156 – 2165.
[67] A. Violi, T. N. Truong, A. F. Sarofim, *J. Phys. Chem. A* **2004**, *108*, 4846 – 4852.
[68] D. F. Nava, M. B. Mitchell, L. J. Stief, *J. Geophys. Res. A* **1986**, *91*, 4585 – 4589.
[69] Chemical Kinetics Database, NIST Standard Reference Database 17, (Web version), Release 1.4.2, Data version 08.09. http://kinetics.nist.gov/.
[70] K. J. Mintz, D. J. Leroy, *Can. J. Chem.* **1978**, *56*, 941 – 949.
[71] L. N. Krasnoperov, J. P. Peng, P. Marshall, *J. Phys. Chem. A* **2006**, *110*, 3110 – 3120.
[72] M. K. Sabbe, M. Saeys, M. F. Reyniers, G. B. Marin, V. Van Speybroeck, M. Waroquier, *J. Phys. Chem. A* **2005**, *109*, 7466 – 7480.
[73] M. K. Sabbe, F. De Vleeschouwer, M. F. Reyniers, M. Waroquier, G. B. Marin, *J. Phys. Chem. A* **2008**, *112*, 12235 – 12251.

Received: July 2, 2009
Published online on November 26, 2009

